ESEC PROCEEDING
Environmental Science and Engineering Conference
Vol 3, No. 1, November 2022, pp. 51-58
Halaman Beranda Jurnal: http://esec.upnvjt.com/

Investigation of Natural Product Extracts as Green Corrosion Inhibitors on Steels and Alloys: Experimental and Theoretical Approach

Muhamad Akrom* and Wahyu Aji Eko Prabowo

Research Center for Materials Informatics, Faculty of Computer Science, Dian Nuswantoro University, Semarang 50131, Indonesia

Corresponding author: m.akrom@dsn.dinus.ac.id

Kata Kunci:
baja, ekstrak tanaman, inhibitor korosi, metode eksperimen, metode teoritis

ABSTRAK

Ekstrak produk alam menunjukkan kinerja yang sangat baik sebagai green inhibitor korosi pada paduan baja dengan performa inhibisi yang tinggi. Metode eksperimental dan teoritis mampu bersinergi dalam menyelidiki kinerja penghambatan korosi. Laporan ini merupakan literatur komparatif untuk pengembangan inhibitor berbasis bahan alam. Pengembangan penyelidikan ke depan diharapkan dapat menunjukkan interaksi molekul ekstrak tanaman dengan permukaan logam pada tingkat atomik, sehingga diperoleh pemahaman yang sistematis dan detail tentang mekanisme penghambatan korosi pada logam.

Keyword:
steel, plant extract, corrosion inhibitor, experimental methode, theoretical method

ABSTRACT

Natural plant extracts show excellent performance as green corrosion inhibitors on steel with high inhibition efficiency. Experimental and theoretical methods are able to synergize in investigating corrosion inhibition performance. This report is a comparative literature for the development of natural-based inhibitors. The development of future investigations is expected to show the interaction of plant extract molecules with metal surfaces at the atomic level, so that a systematic and detailed understanding of the mechanism of corrosion inhibition in metal is obtained.

1. INTRODUCTION

Corrosion is decreasing quality (physical and mechanical properties) and the useful life of a material naturally due to an electrochemical reaction. The NACE reports that the global treatment fee for corrosion reaches $2.5 trillion per year (Groenenboom et al., 2017; Koch et al., 2016). Over the last decade these costs have continued to increase (DorMohammadi et al., 2018). Corrosion not only causes economic losses, but also other aspects such as environmental damage, security and safety threats (Chen et al., 2021; Sedik et al., 2020).

Nowadays, inhibitor technology is the best solution in inhibiting the corrosion process. Corrosion inhibitor technology can reduce costs up to 35% or about 875 billion dollars per year (Marzorati et al., 2019). The inhibitor is the chemical compound that in small quantities may provide broad protection when added to a corrosive environment (Ash & Ash, 2000). Corrosion inhibitors play a role in maintaining the useful life of a material, contamination of a material, safety from accidents due to corroded material, and also the production power of a material by inhibiting the activity of the corrosion rate (Akrom et al., 2021).

This review provides an overview of novel report on the use of green corrosion inhibitors on steel surfaces based on experimental and theoretical investigations. This report can provide relational literature for the perfection and utilization of natural products as green inhibitors in metals.

2. MATERIAL AND METHOD

2.1 Natural Extract as Green Corrosion Inhibitor

Investigations of inhibitors continue to grow, especially in the exploration of organic inhibitors based on natural products. This is because inorganic inhibitors are toxic, environmentally unfriendly, and expensive. Natural plant extracts appear as green inhibitors because they are eco-friendly, biodegradable, renewable, do not cause toxins and pollutants, are easy to produce and apply, have high cost effectiveness, and have and are able to provide protection from an environment with a very high level of corrosiveness (Kumar & Yadav, 2021; Vorobyova & Skiba, 2020).

Generally, green inhibitors which in their structure conceive heteroatomic atoms (e.g O, N, S, P) and aromatic rings are effective and efficient as corrosion inhibitors (Popoola, 2019; Stiadi et al., 2019).

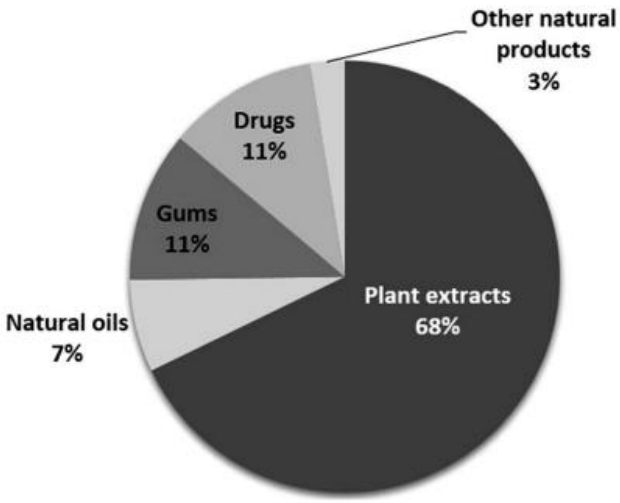

Figure 1. Distribution of Natural Products as Corrosion Inhibitors (Fayomi et al., 2019)

Various recent studies on the utilize of natural products as green inhibitors show positive performance of natural plant extract inhibitor molecules. It was reported that flavanone extract from the yellow plant (Murraya koenigii linn) was investigated as inhibitor in steel with a maximum inhibition efficiency of 98.13% (H. Kumar & Yadav, 2021). Protocatechuic extract of the primrose (Primula vulgaris) plant resulted in a maximum inhibition efficiency of 94.4% on steel (Majd et al., 2019). Eugenol extract of the clove plant (Syzigium aromaticum) showed performance as a corrosion inhibitor on steel with a maximum inhibitory performance of 92.4% (Hnini et al., 2004).

Based on Table 1, it can be observed that, natural plant extract green inhibitors have very good performance with high inhibition efficiency or inhibition efficiency (EI) on steel corrosion in an acidic environment. Inhibition efficiency is a parameter to measure the inhibitor's ability to protect metal surfaces based on the level of corrosion activity reduction (Pramudita et al., 2018).

Table 1. Green Inhibitor on Steel with Concentration of 1000 ppm in 1 M HCl Medium

Green Inhibitor	Inhibition Efficiency (%)
Ananas comosus	98
Pineapple stem	97
Poinciana pulcherrima	96
Primula vulgaris flower	96
Plantago	94
Juglans regia	94
Plantago ovata	94
Cassia occidentalis	93
Mangifera indica leaves	92
Papaia	92
Chinese gooseberry fruit	92
Datura stramonium	91
Cryptocarya nigra	91
Calotropis procera	89
Luffa cylindrica	88
Xantan gum	82
Tinospora crispa	80

2.2 Experimental Investigations

The mechanism of corrosion and corrosion inhibition has been studied extensively through experimental approachs (e.g electrochemical impedance spectroscopy (EIS), potentiodynamic polarization, and gravitational analysis).

2.2.1 Gravimetric Analysis

Gravimetric analysis is also referred to as the weight loss method, because it is based on calculating the difference in weight of the metal during immersion with and without an inhibitor in a corrosive medium. In this gravimetric method, the corrosion rate (CR) can be enumerated by the following equation:

$$CR = \frac{KW}{AT\rho} \quad (1)$$

where CR, K, W, A, T, and ρ are corrosion rate (mmpy), corrosion rate constant, mass difference (mg), surface area (mm^2), immersion time (year), and density (mg/mm^3), while the inhibition efficiency (EI) is:

$$EI(\%) = (1 - \frac{CRp}{CRa}) \times 100\% \quad (2)$$

$$EI(\%) = (1 - \frac{Wp}{Wa}) \times 100\% \quad (3)$$

where CRp and CRa are corrosion rates with and without inhibitor, Wp, and Wa are mass loss in presence and absence of inhibitor, respectively.

Based on Table 2 and Figure 2, it can be seen that the inhibitor of the Amni visnaga plant extract was able to inhibit steel corrosion. the corrosion rate decreased with the addition of inhibitor concentration, indicating an increase in inhibition efficiency. This conduct can be featured to an increase in the contact area of inhibitor with the surface, thereby reducing the reaction site among the steel and the electrolite medium (C. B. P. Kumar et al., 2020; Majd et al., 2019; Popoola, 2019).

E-ISSN: 2798-6241; P-ISSN: 2798-6268 Vol 3, November 2022

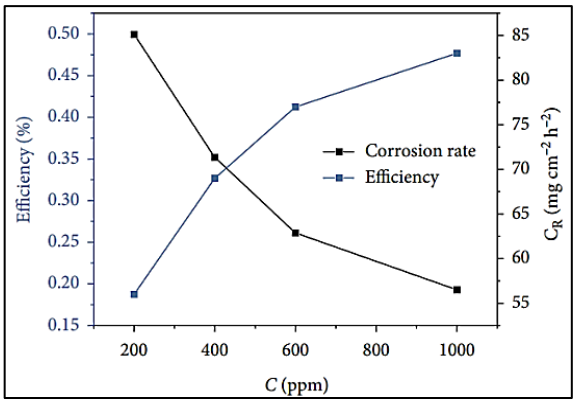

Figure 2. Corrosion Rate and Inhibition Efficiency with and without Amni Visnaga Methanolic Extract as Inhibitor (Zaher et al., 2020)

Table 2. Gravimetric Analysis for Steel in 1 M HCl Medium in Presence and Absence of Amni Visnaga (EMG) Methanolic Extract as Inhibitor (Zaher et al., 2020)

Inhibitor	Concentration (g/L)	Corrosion rate (mg/cm^2 h)	Inhibition efficiency (%)
Blank	-	1.135	-
EMG	0.2	0.4995	56
	0.4	0.3519	69
	0.6	0.2611	77
	1	0.1929	83

2.2.2 Potentiodynamic Polarization

The inhibition rate may also be diligent based on the parameters of the current density that appears on the metal surface using potentiodynamic polarization method. In metal materials that interact with a corrosive medium, oxidation and reduction reactions will occur simultaneously, so that there is an anodic current equal to the cathodic current due to the potential difference between the metal and the electrolyte solution/corrosive medium. The resulting potential difference is a corrosion potential (E_{corr}) and the resulting electric current is a corrosion current (I_{corr}).

$$EI(\%) = (1 - \frac{i'corr}{icorr}) \times 100\% \quad (4)$$

where i'_{corr} and i_{corr} are corrosion current density in presence and absence of inhibitor, respectively. Linear extrapolation from the polarization curve to the corrosion potential is carried out to calculate the current density.

Based on the data in Table 3, we know that the addition of inhibitor concentration of Dardagan fruit extract was able to reduce the anodic dissolution reaction rate (b_a) and the cathodic reduction reaction rate (b_c). The inhibition efficiency (η) increases as corrosion current decreases (i_{corr}). In Figure 3, it can be seen that there is a shift in the polarization curve towards a lower corrosion current along with the addition of inhibitor concentration. Increasing the inhibitor concentration reduces the current density, the corrosion rate decreases, and the inhibition efficiency increase. This is in consequence of the adsorption mechanism of the inhibitor and the larger surface coverage so that it can block the steel surface active sites with a corrosive environment (C. B. P. Kumar et al., 2020; Sedik et al., 2020; Vorobyova & Skiba, 2020).

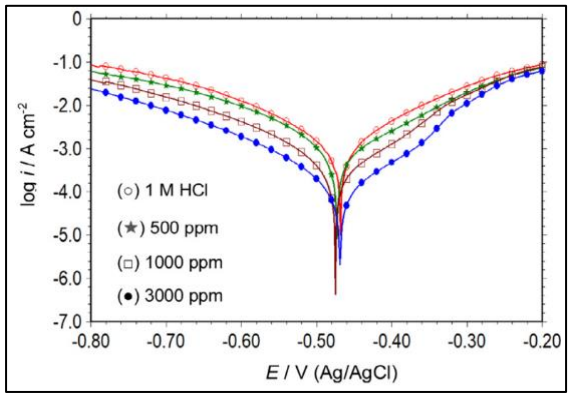

Figure 3. Polarization Curve Variation on Steel corrosion with and without Dardagan Fruit Extract Inhibitor (Sedik et al., 2020)

Table 3. Analysis of Polarization for Steel in 1 M HCl Medium in Presence and Absence of Dardagan Fruit Extract as Inhibitor (Sedik et al., 2020)

C_{inh} (ppm)	E_{corr} (V)(Ag/AgCl)	b_c (mV dec^{-1})	b_a (mV dec^{-1})	i_{corr} (μA cm^{-2})	η (%)
Blank	−0.468	−120	118	1140.1	-
100	−0.464	−128	115	507.3	55.5
500	−0.473	−123	106	563.9	50.5
1000	−0.475	−123	86	203.2	82.2
2000	−0.475	−117	88	168.7	85.2
3000	−0.469	−121	85	89.9	92.1

2.2.3 Electrochemical Impedance Spectroscopy (EIS)

EIS method is commonly used to investigate the performance of an inhibitor.

$$EI(\%) = (1 - \frac{Rp'}{Rp}) \times 100\% \quad (5)$$

where Rp' and Rp are the charge transfer resistance in presence and absence of the inhibitor.

One of the corrosion parameters that is also very important is the charge transfer resistance (Rct), that shows the ability of an inhibitor to inhibit the charge transfer between metal and a corrosive medium. From Table 4, we know that with the increase in inhibitor concentrations, the charge transfer resistances also increases. An increase in the value of the charge transfer resistance an increased charge transfer resistance indicates an increase in corrosion inhibition efficiency. From Figure 4, the Nyquist diagram forms a semi-circular loop.

In the presence of inhibitors, loop widening occurs. The deformation indicates that there is an influence on the charge transfer process owing to the establishment of a protective layer. From the Bode diagram, it can be seen that the phase angle deviates from the 90° shape, as the inhibitor is added, the phase angle increases. the adsorption ability and coverage of the protective layer increase due to the increase in inhibitor concentration, leads to good corrosion inhibition.

Table 4. Electrochemical for Steel in 1 M HCl Medium in Presence and Absence of Xanthene Inhibitor (NAR) (Arrousse et al., 2020)

Medium	Conc (M)	R_s (Ω cm^2)	R_{ct} (Ω cm^2)	Q (μF S^{n-1})	n_{dl}	C_{dl} (μF cm^{-2})	η_{Rct}%
1 M HCl	–	1.037±0.021	49.9 ± 0.15	456.6 ± 0.064	0.8456±0.010	228.9	–
NAR	10^{-4}	3.291±0.015	705.6 ± 2.011	35.91±0.031	0.7901±0.005	13.53	**93**
	10^{-5}	1.666±0.014	223.3 ± 3.006	145.1 ± 0.037	0.8586±0.035	82.49	78
	10^{-6}	1.718±0.013	198.6 ± 1.012	158.2 ± 0.035	0.8931±0.005	104.6	72
	10^{-7}	1.314±0.015	150.2 ± 1.019	299.8 ± 0.054	0.8878±0.009	202.6	67

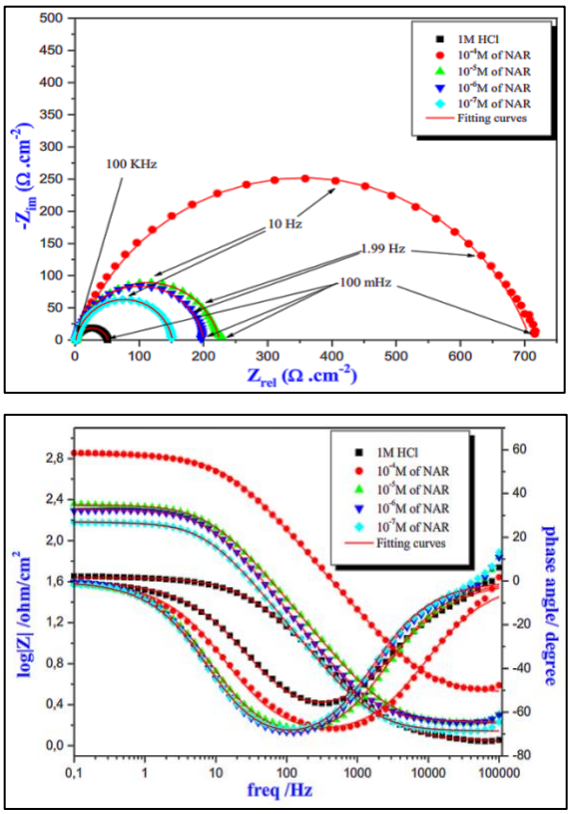

Figure 4. Plot of Nyquist and Bode on Variation of NAR Inhibitor Concentration (Arrousse et al., 2020)

2.3 Theoretical Investigations

In quantum mechanics, interactions in material systems involve electrons and nuclei. The material system is represented as a wave function (ψ). Generally, the Schrödinger equation is used as an approximation to solving the wave function of medest particle systems. In plentiful particle systems, a more proper approach is behooved. One of the right approaches is the density functional theory (DFT). The DFT method is a refinement of the initial Hohenberg-Kohn, which assumes that the total energy is a electron density functional.

$$E(\rho) = Ts(\rho) + J(\rho) + V_{ext}(\rho) + E_{nuc}(\rho) + E_{xc}(\rho) \quad (6)$$

where Ts(ρ) is the kinetic energy, J(ρ) is the potential energy, $V_{ext}(\rho)$ is the electron-ion potential, $E_{nuc}(\rho)$ is the ion-ion potential, and $E_{xc}(\rho)$ is an exchange-correlation functionoal.

Density functional theory (DFT) is widely applied to predict the electronic and structural properties of materials, as well as the interactions between materials. DFT is a quantum mechanical calculation method based on the electron density, the electron density, comprises very prominent and specific information at the atomic scale regarding the characteristics of the material system in its ground state (Verma, 2018).

2.3.1 Molecular Orbitals

Frontier molecular orbitals (FMO) plots describe the distribution of electron density that can be utilized to predict the active site of the inhibitor. The highest occupied molecular orbital (HOMO) is the highest occupied molecular orbital with electrons, which describes the ability of the inhibitor molecule as an electron donor. The lowest unoccupied molecular orbital (LUMO) is the lowest unoccupied molecular orbital, which describes the ability of inhibitor molecules as electron acceptors (Hadisaputra et al., 2019).

Based on Figure 5, the scatter of electron density inclines to be confined around the two oxygen atoms and the aromatic ring, indicating the propensity of the HOMO area as an electron donor, purpose that this section of the atom is held to be the active site, while the scatter of electron density in the LUMO area, inclines to be deployment over the carbon chain and the benzene cycle, purpose to be the electron acceptor region.

The distribution of electron density in the HOMO-LUMO region also shows that the molecular mechanism of the inhibitor molecule can be through the lone pair of electrons from the oxygen atom and/or the π-electrons of the benzene ring. This explains that the potential interaction of inhibitor molecules with metal surfaces tends to be through a donor-acceptor mechanism. The inhibitor molecule is not only an electron donor to the metal surface, but also acts as an electron acceptor from the metal surface.

The HOMO-LUMO orbital can also show the presence of electron transfer based on its energy value (Marni et al., 2019). A high E_{HOMO} exhibites a good potential as an electron donor, while the low E_{LUMO} value exhibites a good potential as an electron acceptor (Gece & Bilgiç, 2017). The gap energy (E_{gap}) exhibites the potential ability of molecules to bond with metal surfaces.

$$E_{gap} = E_{LUMO} - E_{HOMO} \quad (7)$$

A lower gap energy exhibites that the inhibitor has a high level of chemical reactivity, which associated to the inhibition performance (TÜZÜN, 2019; Ammouchi et al., 2020).

In Table 5, it can be seen that Artichoke, Chamomile flower, and Thymus vulgaris have high E_{HOMO}, low E_{LUMO}, and low Egap values. This shows that the three inhibitor molecules have excellent potential as green corrosion inhibitors.

Table 5. HOMO-LUMO Orbitals of Inhibitors

Molecule	HOMO	LUMO
Artichoke	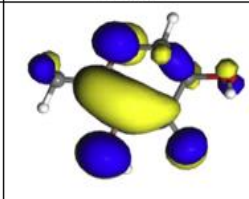	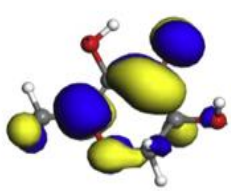
Chamomile flower	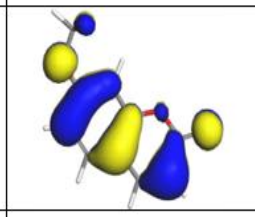	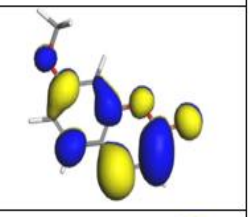
Thymus vulgaris	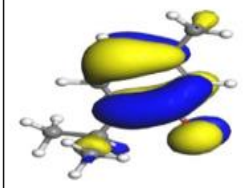	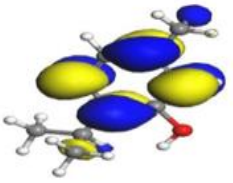

Table 6. Orbital Energy of Inhibitors

Green Inhibitor	E_{HOMO}	E_{LUMO}	E_{gap}
Artichoke	-6.430	-3.086	3.344
Chamomile flower	-5.547	-2.632	2.915
Thynus vulgaris	-5.225	-0.818	4.407

2.3.2 Quantum Chemical (QC) Parameters

QC parameter calculations were conducted to gain a relation of the electronic properties with the inhibition performance. The quantum descriptors basically indicates the level of chemical reactivity. Chemical reactivity is associated to the potential for corrosion inhibition or corrosion inhibition efficiency. High chemical reactivity indicates excellent corrosion inhibition potential or high inhibition efficiency of inhibitor molecules (C. B. P. Kumar et al., 2020), since the inhibitor molecule has the potential to easily interact and form bonds with the surface (Farahati et al., 2020; Marni et al., 2019), and and the inhibitor has a wider contact area with the metal surface (Anupama & Joseph, 2018; Daouda et al., 2019). Molecules that have high chemical reactivity have excellent potential as green inhibitors.

The descriptors above include ionization potential (I), electron affinity (A), absolute electronegativity (χ), dipole moment (μ), global hardness (η), global softness (σ), electrophilicity (ω), nucleophilicity (ε), fraction of electrons transferred (ΔN), and electron back-donation ($\Delta E_{back\text{-}donation}$). The low ionization potential and high electron affinity indicate that the molecule has high reactivity. Electronegativity is cohesive to the capability of the inhibitor to attract electrons, till electron balance is accomplished. Low electronegativity values indicate high reactivity. Hardness and softness denote the resistance to transfer and a capacity to accept charge, respectively. Low hardness and high softness values represent high reactivity. Dipole moment depicts the allocation of electrons in the molecular structure. A high dipole moment value indicates high reactivity. Electrophilicity portrays the aptitude of a molecule to permeate electrons. Low electrophilicity denotes high reactivity. Electron back-donation is a charge transfer followed by a back-donation. A more negative value of Eback-donation exhibits better inhibition performance. The interaction of the inhibitor molecule and the metal surface is characterized by the fraction of electrons transferred. Electronegativity differences between the molecule and the metal surface cause electron transfer (El Hassani et al., 2020).

$$I = -E_{HOMO} \quad (8)$$

$$A = -E_{LUMO} \quad (9)$$

$$\chi = \frac{I + A}{2} \quad (10)$$

$$\eta = \frac{I - A}{2} \quad (11)$$

$$\sigma = \frac{1}{\eta} \quad (12)$$

$$\mu = -\chi \quad (13)$$

$$\omega = \frac{\mu^2}{2\eta} \quad (14)$$

$$\varepsilon = \frac{1}{\omega} \quad (15)$$

$$\Delta E_{back-donation} = -\frac{\eta}{4} \quad (16)$$

$$\Delta N = \frac{\chi met - \chi inh}{2(\eta met + \eta inh)} \quad (17)$$

where χ_{met} is electronegativity of metal and χ_{inh} is electronegativity of inhibitor, while η_{met} and η_{inh} are the hardness of the metal and inhibitor, respectively.

Table 7. Quantum Chemical Parameters of Green Inhibitor Compounds Inhibition

Green Inhibitor	A	I	χ	η	ΔN
Artichoke	3.086	6.430	4.758	1.672	0.0185
Chamomile flower	2.632	5.547	4.089	1.457	0.2508
Thynus vulgaris	0.818	5.225	3.021	2.203	0.4083

Based on Table 6, the inhibitors above appear to kind of chemical reactivity, and exhibit excellent interaction potential on metal surfaces, making them a potential good as green corrosion inhibitors.

E-ISSN: 2798-6241; P-ISSN: 2798-6268 Vol 3, November 2022

3. RESULT AND DISCUSSIONS

3.1 Corrosion Mechanism

The corrosion process takes place naturally, but can be controlled, thus the material degradation process can be slowed down.

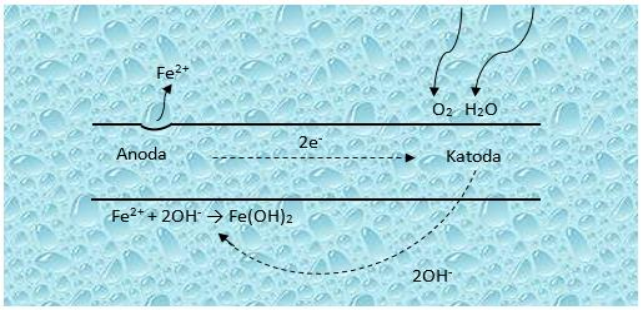

Figure 5. Mechanism of Corrosion of Iron in a Neutral Environment

In general, the corrosion mechanism is similar to the process that takes place in a fuel cell. The surface of the corroded iron acts like a mixed electrode (anode and cathode) which is electrically connected through the iron body itself, where anodic and cathodic reactions occur on the surface. Corrosion reaction is an electrochemical reaction consisting of anodic and cathodic reactions.

In an oxidation reaction in anode, a metal is oxidized by giving up electrons to form positive metal ions (cations). The positive metal atoms escape from the metal surface as ions and into the electrolyte solution in a corrosive environment. Positive metal ions migrate through the electrolyte from the anode to the cathode. This oxidation reaction also releases electrons that can move from the anode to the cathode through an electrical connection (the iron body itself). A stream of electrons flows towards the cathode, acting as an electric current). In a reduction reaction, electrons are captured by dissolved oxygen and/or water molecules. Oxygen dissolved in water will be reduced to negative ions (anions). Negative ions flow (diffuse) from the anode to the cathode through the electrolyte.

From Figure 6, in a neutral environment, ferrous metal undergoes an oxidation reaction by releasing electrons to form Fe^{2+} metal ions. The ions escape to the electrolyte medium from the iron surface, then migrate from the anode to the cathode. The electrons can move from the anode to the cathode through an electrical connection (the iron body itself). Furthermore, in the reduction reaction, electrons are captured by dissolved oxygen. Oxygen is reduced to a negative ion (anion) OH^-. Negative ions flow (diffuse) from the cathode to the anode through the electrolyte. Fe^{2+} ions and OH^- ions will form $Fe(OH)_2$ precipitates. As a result of further oxidation, $Fe(OH)_2$ will form rust products such as Fe_2O_3, Fe_3O_4, and also FeOOH. In an acidic environment, the relatively large number of H^+ ions allows other reduction reactions such as hydrogen evolution to occur. The existence of two reactions that take place at the cathode causes the iron metal to be oxidized more. This explains why corrosion in an acidic environment is greater than in a neutral environment (Verma, 2018). It has been widely reported that the presence of moisture and oxygen favors the formation of more OH^- as a component of rust formation (Ahmad, 2003).

Corrosion reaction in acid medium:

Oxidation: $2Fe \rightarrow 2Fe^{2+} + 4e^-$

Reduction: $O_2 + 4H^+ + 4e^- \rightarrow 2H_2O$

Reaction: $2Fe + O_2 + 4H^+ \rightarrow 2Fe^{2+} + 2H_2O$

$4Fe^{2+} + 4H_2O + 3O_2 \rightarrow 2Fe_2O_3 + 4H_2O$

Corrosion reaction in alkaline medium:

Oxidation: $2Fe \rightarrow 2Fe^{2+} + 4e^-$

Reduction: $O_2 + 2H_2O + 4e^- \rightarrow 4OH^-$

Reaction: $2Fe + O_2 + 2H_2O \rightarrow 2Fe^{2+} + 4OH^- \rightarrow 2Fe(OH)_2$

$4Fe(OH)_2 + O_2 + 2H_2O \rightarrow 4Fe(OH)_3$

$2Fe(OH)_3 \rightarrow Fe_2O_3 + 3H_2O$

3.2 Inhibition Mechanism

The mechanism of corrosion inhibition may involve chemical and/or physical adsorption processes to establish atomic orbitals (adsorbed layer, protective layer, complex compound) among the inhibitor and surface. The adsorption of inhibitor at the interface with the metal allows 4 adsorption mechanisms to occur, namely: (a) electrostatic interactions between molecules and metals, (b) interactions between electron pairs and metals, (c) interactions between π-electrons and metals, and (d) a combination of these three mechanisms. The adsorption is also largely determined by the planarity of the molecules and the lone pairs of electrons present in the heteroatom group (C. B. P. Kumar et al., 2020).

The effectiveness of natural plant extract compounds as inhibitors depend on their capability to establish protective layers on metal surfaces that can avert charge and mass transfer, thereby protecting and separating metals from the corrosive environment (Dehghani et al., 2020; Fayomi et al., 2019).

The formation of the adsorbed layer depends on the ability of the lone pair donor-acceptor and/or the interaction between the π-electrons of the aromatic ring of the inhibitor with the vacant d-orbital of the surface atom, both of which facilitate the formation of the adsorbed layer by coordinating covalent bonds (Aliofkhazraei, 2014; Arrousse et al., 2020; Zaher et al., 2020). In general, the heteroatom group acts as an adsorption center that interacts with the surface, because the inhibitor may not be completely adsorbed on the surface, but can occupy the active site to inhibit the oxidation or reduction reaction, so that the corrosion process will decrease due to the active site. covered by the adsorbed inhibitor (Arthur & Abechi, 2019).

The constancy to establish complex compounds of the molecule and metal surfaces can also be confirmed based on the adsorption energy. Adsorption energy is related to the stability of the complex layer formation.

$$E_{ads} = E_{inh/surf} - (E_{inh} + E_{surf}) \quad (18)$$

where $E_{inh/surf}$ is the total energy between the surface and the adsorbed inhibitor, E_{inh} is the total energy of the inhibitor, E_{surf} is the total energy of the surface, and E_{ads} is the adsorption energy.

From Table 7, we know that the adsorption energy of Artichoke, Chamomile flower, and Thymus vulgaris extracts as a green inhibitor, was energetically strong and related to the inhibition performance acquired experimentally.

Table 8. Adsorption Energy of Inhibitors on Steel Surfaces

Green Inhibitor	E_{ads} (kcal/mol)	Inhibition Efficiency (%)	Ref.
Artichoke	-115.90	98.7	(Salmasifar et al., 2021)
Chamomile flower	-111.17	97	(Shahini et al., 2021)
Thymus vulgaris	-90.67	95	(Lashgari et al., 2021)

4. CONCLUSION

Natural plant extracts show excellent performance in inhibiting steel corrosion, where the corrosion inhibition efficiency is very high. Experimental and theoretical methods are able to synergize in investigating corrosion inhibition performance.

ACKNOWLEDGEMENT

There is no conflict of interest concerning the publication of this article.

REFERENCES

Ahmad, S. (2003). Reinforcement corrosion in concrete structures, its monitoring and service life prediction - A review. Cement and Concrete Composites, 25(4-5 SPEC), 459–471.

Aliofkhazraei, M. (2014). Developments in Corrosion Protection. In Developments in Corrosion Protection

Ammouchi, N., Allal, H., Belhocine, Y., Bettaz, S., & Zouaoui, E. (2020). DFT computations and molecular dynamics investigations on conformers of some pyrazinamide derivatives as corrosion inhibitors for aluminum. Journal of Molecular Liquids, 300, 112309

Anupama, K. K., & Joseph, A. (2018). Experimental and Theoretical Studies on Cinnamomum verum Leaf Extract and One of Its Major Components, Eugenol as Environmentally Benign Corrosion Inhibitors for Mild Steel in Acid Media. Journal of Bio- and Tribo-Corrosion, 4(2), 0

Arrousse, N., Salim, R., Kaddouri, Y., zarrouk, A., Zahri, D., Hajjaji, F. El, Touzani, R., Taleb, M., & Jodeh, S. (2020). The inhibition behavior of two pyrimidine-pyrazole derivatives against corrosion in hydrochloric solution: Experimental, surface analysis and in silico approach studies. Arabian Journal of Chemistry, 13(7), 5949–5965

Arthur, D. E., & Abechi, S. E. (2019). Corrosion inhibition studies of mild steel using Acalypha chamaedrifolia leaves extract in hydrochloric acid medium. SN Applied Sciences, 1(9), 1–11

Ash, M., & Ash, I. (2000). Handbook of Corrosion inhibitors. In Metal Finishing (Vol. 98, Issue 10)

Chen, X., Chen, Y., Cui, J., Li, Y., Liang, Y., & Cao, G. (2021). Molecular dynamics simulation and DFT calculation of "green" scale and corrosion inhibitor. Computational Materials Science, 188(August 2020), 110229.

Daouda, D., Douadi, T., Ghobrini, D., Lahouel, N., & Hamani, H. (2019). Investigation of some phenolic-type antioxidants compounds extracted from biodiesel as green natural corrosion inhibitors; DFT and molecular dynamic simulation, comparative study. AIP Conference Proceedings, 2190.

Dehghani, A., Mostafatabar, A. H., Bahlakeh, G., & Ramezanzadeh, B. (2020). A detailed study on the synergistic corrosion inhibition impact of the Quercetin molecules and trivalent europium salt on mild steel; electrochemical/surface studies, DFT modeling, and MC/MD computer simulation. Journal of Molecular Liquids, 316, 113914.

DorMohammadi, H., Pang, Q., Árnadóttir, L., & Burkan Isgor, O. (2018). Atomistic simulation of initial stages of iron corrosion in pure water using reactive molecular dynamics. Computational Materials Science, 145, 126–133.

El Hassani, A. A., El Adnani, Z., Benjelloun, A. T., Sfaira, M., Benzakour, M., Mcharfi, M., Hammouti, B., & Emran, K. M. (2020). DFT Theoretical Study of 5-(4-R-Phenyl)-1H-tetrazole (R = H; OCH3; CH3; Cl) as Corrosion Inhibitors for Mild Steel in Hydrochloric Acid. Metals and Materials International, 26(11), 1725–1733.

Farahati, R., Behzadi, H., Mousavi-Khoshdel, S. M., & Ghaffarinejad, A. (2020). Evaluation of corrosion inhibition of 4-(pyridin-3-yl) thiazol-2-amine for copper in HCl by experimental and theoretical studies. Journal of Molecular Structure, 1205, 127658.

Fayomi, O. S. I., Akande, I. G., & Nsikak, U. (2019). An Overview of Corrosion Inhibition using Green and Drug Inhibitors. Journal of Physics: Conference Series, 1378(2), 0–7.

Gece, G., & Bilgiç, S. (2017). A computational study of two hexitol borates as corrosion inhibitors for steel. International Journal of Corrosion and Scale Inhibition, 6(4), 476–484.

Groenenboom, M. C., Anderson, R. M., Horton, D. J., Basdogan, Y., Roeper, D. F., Policastro, S. A., & Keith, J. A. (2017). Doped Amorphous Ti Oxides to Deoptimize Oxygen Reduction Reaction Catalysis. Journal of Physical Chemistry C, 121(31), 16825–16830.

Hadisaputra, S., Purwoko, A. A., Hakim, A., Savalas, L. R. T., Rahmawati, R., Hamdiani, S., & Nuryono, N. (2019). Ab initioMP2 and DFT studies of ethyl-p-methoxycinnamate and its derivatives as corrosion inhibitors of iron in acidic medium. Journal of Physics: Conference Series, 1402(5).

Hnini, K., Chtaini, A., & Elbouadili, A. (2004). Inhibition of metallic corrosion with eugenol. Bulletin of Electrochemistry, 20(11), 481–485.

Koch, G., Varney, J., Thompson, N., Moghissi, O., Gould, M., & Payer, J. (2016). International Measures of Prevention, Application, and Economics of Corrosion Technologies Study. NACE International, March 1, 2016, 216.

Kumar, C. B. P., Prashanth, M. K., Mohana, K. N., Jagadeesha, M. B., Raghu, M. S., Lokanath, N. K., Mahesha, & Kumar, K. Y. (2020). Protection of mild

steel corrosion by three new quinazoline derivatives: experimental and DFT studies. Surfaces and Interfaces, 18(October 2019), 100446.

Kumar, H., & Yadav, V. (2021). Highly efficient and eco-friendly acid corrosion inhibitor for mild steel: Experimental and theoretical study. Journal of Molecular Liquids, 335, 116220.

Lashgari, S. M., Bahlakeh, G., & Ramezanzadeh, B. (2021). Detailed theoretical DFT computation/molecular simulation and electrochemical explorations of Thymus vulgaris leave extract for effective mild-steel corrosion retardation in HCl solution. Journal of Molecular Liquids, 335, 115897.

Majd, M. T., Asaldoust, S., Bahlakeh, G., Ramezanzadeh, B., & Ramezanzadeh, M. (2019). Green method of carbon steel effective corrosion mitigation in 1 M HCl medium protected by Primula vulgaris flower aqueous extract via experimental, atomic-level MC/MD simulation and electronic-level DFT theoretical elucidation. Journal of Molecular Liquids, 284, 658–674.

Marni, L. G., Emriadi, E., Syukri, S., & Imelda, I. (2019). Mempelajari inhibisi korosi senyawa khellin dan visnagin pada atom besi menggunakan metode DFT (density functional theory). Jurnal Litbang Industri, 9(2), 111.

Marzorati, S., Verotta, L., & Trasatti, S. P. (2019). Green corrosion inhibitors from natural sources and biomass wastes. Molecules, 24(1).

Popoola, L. T. (2019). Organic green corrosion inhibitors (OGCIs): A critical review. Corrosion Reviews, 37(2), 71–102.

Pramudita, M., Sukirno, S., & Nasikin, M. (2018). Rice Husk Extracts Ability to Reduce the Corrosion Rate of Mild Steel. International Journal of Chemical Engineering and Applications, 9(4), 143–146.

Radilla, J., Negrón-Silva, G. E., Palomar-Pardavé, M., Romero-Romo, M., & Galván, M. (2013). DFT study of the adsorption of the corrosion inhibitor 2-mercaptoimidazole onto Fe(1 0 0) surface. Electrochimica Acta, 112, 577–586.

Salmasifar, A., Edraki, M., Alibakhshi, E., Ramezanzadeh, B., & Bahlakeh, G. (2021). Combined electrochemical/surface investigations and computer modeling of the aquatic Artichoke extract molecules corrosion inhibition properties on the mild steel surface immersed in the acidic medium. Journal of Molecular Liquids, 327, 114856.

Sastri, V. S., & Perumareddi, J. R. (1997). Molecular Orbital Theoretical Studies of Some Organic Corrosion Inhibitors. Corrosion (Houston), 53(8).

Sedik, A., Lerari, D., Salci, A., Athmani, S., Bachari, K., Gecibesler, H., & Solmaz, R. (2020). Dardagan Fruit extract as eco-friendly corrosion inhibitor for mild steel in 1 M HCl: Electrochemical and surface morphological studies. Journal of the Taiwan Institute of Chemical Engineers, 107(xxxx), 189–200.

Shahini, M. H., Keramatinia, M., Ramezanzadeh, M., Ramezanzadeh, B., & Bahlakeh, G. (2021). Combined atomic-scale/DFT-theoretical simulations & electrochemical assessments of the chamomile flower extract as a green corrosion inhibitor for mild steel in HCl solution. Journal of Molecular Liquids, 342, 117570.

Stiadi, Y., Arief, S., Aziz, H., Efdi, M., & Emriadi, E. (2019). INHIBISI KOROSI BAJA RINGAN MENGGUNAKAN BAHAN ALAMI DALAM MEDIUM ASAM KLORIDA: Review. Jurnal Riset Kimia, 10(1), 51.

TÜZÜN, B. (2019). Investigation of Benzimidazole Derivates as Corrosion Inhibitor by DFT. Cumhuriyet Science Journal, 40(2), 396–405.

Verma, D. K. (2018). Density Functional Theory (DFT) as a Powerful Tool for Designing Corrosion Inhibitors in Aqueous Phase. Advanced Engineering Testing.

Vorobyova, V., & Skiba, M. (2020). Apricot pomace extract as a natural corrosion inhibitor of mild steel corrosion in 0.5 M NaCl solution: A combined experimental and theoretical approach. Journal of Chemical Technology and Metallurgy, 55(1), 210–222.

Zaher, A., Chaouiki, A., Salghi, R., Boukhraz, A., Bourkhiss, B., & Ouhssine, M. (2020). Inhibition of Mild Steel Corrosion in 1M Hydrochloric Medium by the Methanolic Extract of Ammi visnaga L. Lam Seeds. International Journal of Corrosion, 2020.